Au-Functionalized Hematite Hybrid Nanospindles: General Synthesis, Gas Sensing and Catalytic Properties

ARTICLE *in* THE JOURNAL OF PHYSICAL CHEMISTRY C · APRIL 2011

Impact Factor: 4.77 · DOI: 10.1021/jp110421v

8 AUTHORS, INCLUDING:

Jun Zhang
University of Jinan (Jinan, China)
163 PUBLICATIONS **2,981** CITATIONS
SEE PROFILE

Xianghong Liu
Qingdao University
30 PUBLICATIONS **982** CITATIONS
SEE PROFILE

THE JOURNAL OF PHYSICAL CHEMISTRY C

ARTICLE

pubs.acs.org/JPCC

Au-Functionalized Hematite Hybrid Nanospindles: General Synthesis, Gas Sensing and Catalytic Properties

Jun Zhang, Xianghong Liu, Liwei Wang, Taili Yang, Xianzhi Guo, Shihua Wu, Shurong Wang, and Shoumin Zhang*

Department of Chemistry, Nankai University, Tianjin 300071, People's Republic of China

Supporting Information

ABSTRACT: Hybrid nanomaterials combining the properties of different compositions, which may exhibit multiple functions, are of great significance from both scientific and practical perspectives. In this work, an efficient, green, and general strategy has been developed to fabricate Au(Pt)-functionalized α-Fe_2O_3 hybrid nanospindles. The morphology, structure, and composition of the hybrid nanostructures were characterized by means of XRD/TEM/XPS. Inspired by the unique functions of Au and α-Fe_2O_3, we have applied the Au/α-Fe_2O_3 hybrid nanospindles as a multifunctional nanomaterial for gas sensing and CO oxidation. The obtained results demonstrate that, after functionalization with Au nanoparticles, the hybrid nanospindles exhibit much higher activity for both applications compared to pristine α-Fe_2O_3, indicating a great potential for multifunctional applications.

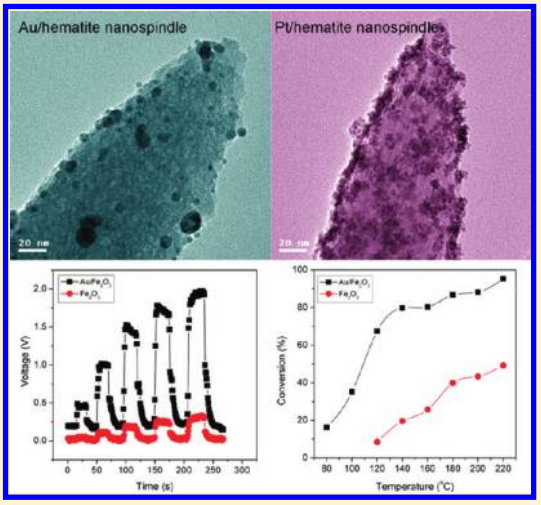

INTRODUCTION

Hybrid nanomaterials, which combine the merits of two or more compositions, have received a great deal of attention for various applications due to their synergy or enhanced properties over their single components.[1−5] Moreover, hybrid nanomaterials, which may exhibit multi-functionalities derived from their compositions, are also of vital significance from the viewpoints of both fundamental research and practical application. In the realm of hybrid nanomaterials, considerable effort has been centered on the noble metals-based systems. Various methods have been developed to immobilize noble metals onto diverse supports to obtain the desired functional nanomaterials. For instance, using a two-step synthesis, preformed metal nanoparticles (NPs) such as Au, Pt, and Pd can be attached onto various support materials with the assistance of a linker reagent like silane coupling agent,[6−11] polyelectrolyte,[12−14] biomolecules,[15−19] and $SnCl_2$.[20,21] In addition, effort has also been made in loading noble metals on TiO_2[22] and CNTs,[23,24] without using any surfactant or linkers. A high-temperature (300 °C) growth method is capable of producing dumbbell-like Au(Pt)/Fe_3O_4 hybrid nanoparticles that are active for cancer therapy, magnetics, optics, oxygen reduction, and CO oxidation.[25−28] Despite the success of the above-mentioned works, their synthetic process may suffer from drawbacks such as multisteps, use of toxic reagent, high fabrication cost, high temperature, and long synthesis time. Therefore, it is still a challenge to develop a facile, green, and cost-effective method to fabricate hybrid nanomaterials.

As an important semiconductor, hematite (α-Fe_2O_3) has been widely investigated for catalyst, pigment, chemical sensor, water treatment, and so on. Due to the tight dependence of properties on the morphology of materials, diverse α-Fe_2O_3 nanostructures have been reported to date, such as nanospindles,[29] nanorods,[30] nanowires,[31] and nanotubes.[32,33] Besides the effect of morphology, the composition of materials also has a significant influence on their properties. On account of their unusual electronic and chemical properties when the particle size decreases to several nanometers, Au NPs have been extensively studied for many areas of application such as catalysis, optics, and electrochemistry.[34−36] The functionalization of α-Fe_2O_3 with Au NPs could provide an opportunity to find new properties and applications. For example, Shevchenko and co-workers demonstrated the optical and supermagnetic performances of a Au@α-Fe_2O_3 core−shell nanostructure obtained from a two-step synthesis.[37] Au nanostructures have been grown on α-Fe_2O_3 nanospindles using a seed-mediated growth to modulate their optical response.[11,38] Furthermore, the sensor and catalyst

Received: November 1, 2010
Revised: January 19, 2011
Published: March 16, 2011

performances of α-Fe_2O_3 can also be significantly enhanced by Au NPs.[19,39,40]

In this contribution, we demonstrate the fabrication of Au NPs-functionalized α-Fe_2O_3 hybrid nanospindles using a facile, green, and one-pot strategy. The nontoxic biocompatible lysine was used as both a linker and capping reagent to anchor Au NPs onto the nanospindles, instead of the widely used toxic chemicals such as silane coupling reagent and polyelectrolyte. This one-pot procedure can also be used to fabricate Pt/α-Fe_2O_3 hybrid nanomaterials, revealing a generality of the method. Most importantly, we found that, after functionalization by Au NPs, the α-Fe_2O_3 nanospindles showed dramatically improved properties for application as both gas sensing material and CO oxidation catalyst, which holds a great potential for practical applications.

EXPERIMENTAL SECTION

Chemicals. $FeCl_3$, NaH_2PO_4, ethanol, lysine, and $NaBH_4$ were of analytical grade and purchased from Guangfu Fine Chemical Research Institute (Tianjin, China). $HAuCl_4 \cdot 4H_2O$ and $H_2PtCl_6 \cdot 6H_2O$ was obtained from Yingdaxigui Chemical Reagent Company (Tianjin, China). Distilled water was used throughout the experiments.

Synthesis of α-Fe_2O_3 Nanospindles. Monodisperse α-Fe_2O_3 nanospindles were prepared according to the literature.[41] An 80-mL portion of aqueous solution containing 2.0×10^{-2} M $FeCl_3$ and 4.5×10^{-4} M NaH_2PO_4 was heated at 100 °C for 72 h. The resulting precipitate was centrifuged and washed several times with water and ethanol, and then dried at 80 °C.

Synthesis of Au(Pt)/α-Fe_2O_3 Hybrid Nanospindles. A 0.2-g portion of α-Fe_2O_3 nanospindles was dispersed in 20 mL of H_2O, followed by the addition of 3 mL of 1.0×10^{-2} M $HAuCl_4$ and 3 mL of 1.0×10^{-2} M lysine. The suspension was stirred for 30 min and then 5 mL of 0.1 M fresh $NaBH_4$ (excess) solution was added to reduce $HAuCl_4$ to metallic Au NPs. After further stirring for about 30 min, the precipitate was collected by centrifugation and washed with water and absolute ethanol and dried at 80 °C. The product was heated at 300 °C for 0.5 h to remove lysine. The synthesis of Pt/α-Fe_2O_3 hybrid nanospindles is similar to that for Au/α-Fe_2O_3, while 5 mL of 7.7×10^{-3} M H_2PtCl_6 was used in stead of $HAuCl_4$.

Characterizations. The crystalline structure of the product was characterized by powder X-ray diffraction (XRD, Rigaku D/max-2500, Cu kα, λ = 1.5418 Å). The morphology of the nanospindles was observed by transmission electron microscope (TEM) and high resolution TEM (HRTEM) on a Philips FEI Tecnai 20ST at an acceleration voltage of 200 kV. The chemical composition of the sample was analyzed by using X-ray photoelectron spectroscopy (XPS, Kratos Axis Ultra DLD spectrometer, Al−Kα X-ray monochromator).

Gas Sensor and CO Oxidation Tests. Gas sensing tests were performed on a commercial HW-30A Gas Sensing Measurement System (HanWei Electronics Co., Ltd., Henan, China) at an operating temperature of 300 °C. The sensor sensitivity is defined as the ratio of R_a/R_g, where R_a and R_g are the electrical resistances of the sensor in air and in test gas, respectively. Details of the sensor fabrication, photograph, and gas sensing test principle can be seen in our previous work.[39] The catalytic activity of the Au NPs-functionalzed α-Fe_2O_3 nanospindles was measured in a fixed-bed stainless-steel tubular reactor using 50 mg catalyst powder. The reaction gas contains 10% CO balanced with air at a total flow rate of 36.3 mL/min. The operation temperature was controlled with a thermocouple placed in the catalyst bed. After 30 min reaction, the effluent gases were analyzed online by a GC-900A gas chromatography with a thermal conductivity detector (TCD). The activity of catalyst was evaluated by the CO conversion.

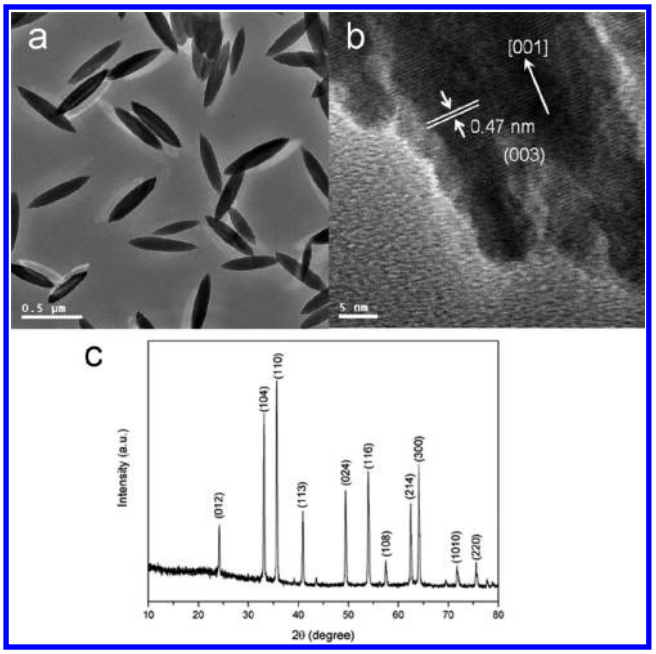

Figure 1. TEM images (a,b) and XRD pattern (c) of the as-synthesized α-Fe_2O_3 nanospindles.

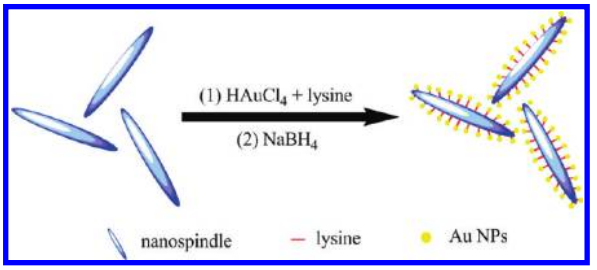

Figure 2. Procedure for the synthesis of Au NPs-functionalized α-Fe_2O_3 nanospindles.

RESULTS AND DISCUSSION

Figure 1 shows the TEM images and XRD pattern of the as-synthesized α-Fe_2O_3 nanospindles. The α-Fe_2O_3 nanoparticles in Figure 1a exhibit a spindle-like morphology with a width of 75−125 nm and length of 350−550 nm. Figure 2b displays the HRTEM image obtained from the tip of a nanospindle. The lattice planes have a space of 0.47 nm of the (003) planes, indicating the nanospindles grow along the [001] direction.[33] The XRD pattern in Figure 1c agrees well with the hematite phase (JCPDS No. 33−0644).

The synthesis for the Au NPs-functionalzed α-Fe_2O_3 nanospindles is illustrated in Figure 2. Different from the conventional two-step method,[6−14] where the support materials should be first functionalized with a functional group such as $-NH_2$ to absorb the preprepared metal NPs, our synthesis requires no prefunctionalization of the nanospindle support. The lysine molecules with two kinds of functional groups ($-NH_2$ and $-COOH$) play

dx.doi.org/10.1021/jp110421v |J. Phys. Chem. C 2011, 115, 5352–5357

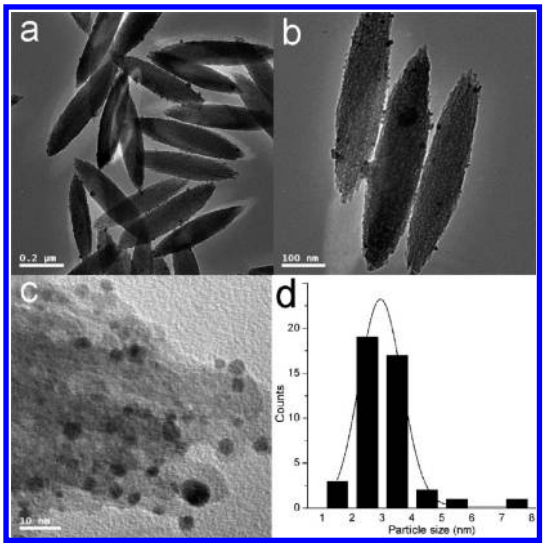

Figure 3. TEM images (a−c) of the Au NPs-functionalized α-Fe_2O_3 nanospindles and size distribution histogram for Au NPs in (c).

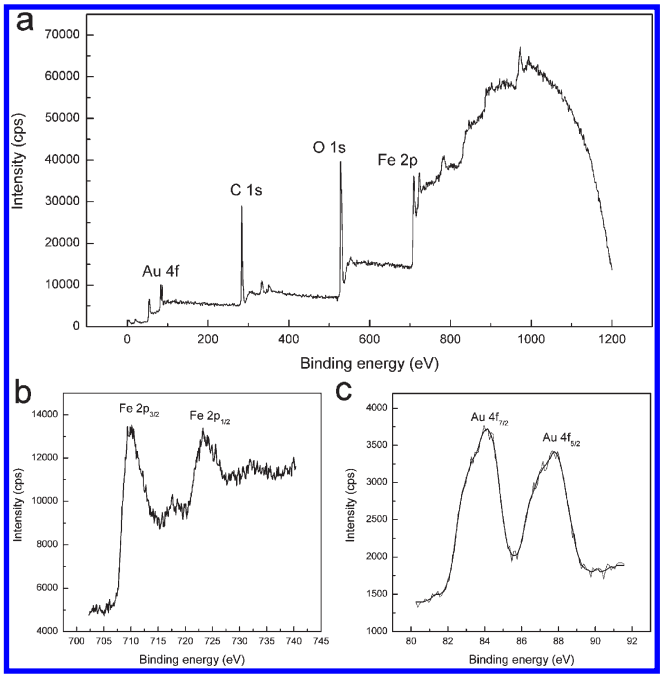

Figure 4. Wide XPS spectrum of Au NPs-functionalized α-Fe_2O_3 nanospindles (a) and high resolution spectrum for Fe 2p (b) and Au 4f (c).

a dual role as both a linker and capping agent.[17] As a linker, the lysine can link Au NPs with α-Fe_2O_3 support due to the strong coordination ability between the functional groups and transition metal ions. As a capping agent, lysine enables the formation of Au NPs with a small size on fast reduction by $NaBH_4$. The Au NPs are formed and simultaneously anchored to α-Fe_2O_3 support in one step, which largely simplifies the synthesis. Also this is a green, user-friendly, and environmentally benign synthesis because no toxic reagents are used.

The TEM images of the Au NPs-functionalized α-Fe_2O_3 nanospindles synthesized using the one-pot procedure are shown in Figure 3a−c. From these pictures, the Au NPs can be seen

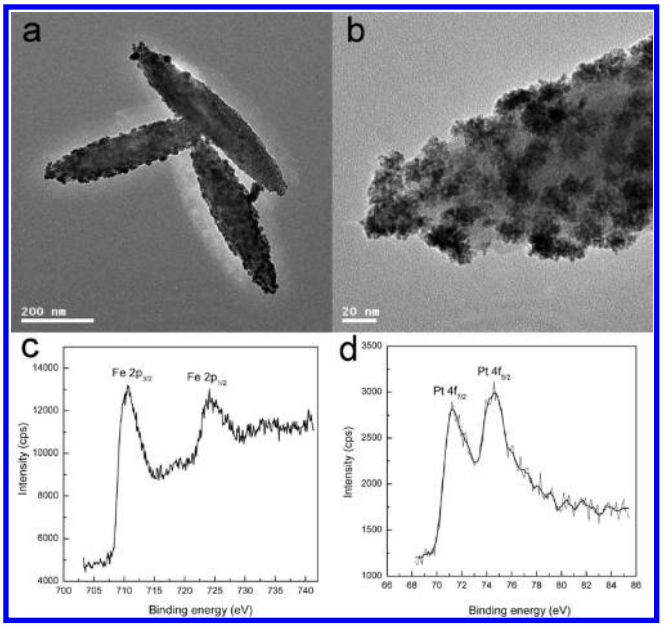

Figure 5. TEM images of Pt-functionalized α-Fe_2O_3 nanospindles (a,b) and high resolution XPS spectrum for Fe 2p (c) and Pt 4f (d).

clearly on the surface of nanospindles. Especially in Figure 3c of a high magnification, the small Au NPs with an average size of ~3 nm can be obviously observed due to their dark image contrast against the support. Figure 4d displays the size distribution histogram for the Au NPs in Figure 3c, revealing a size range of 2−8 nm.

To further confirm the decoration of Au NPs on the α-Fe_2O_3 nanospindles, we have used XPS technique to analyze the surface composition of the hybrids. The XPS spectra are shown in Figure 4. Figure 4a is the wide XPS data, confirming the presence of Au and Fe. The high resolution XPS spectrum for Fe 2p and Au 4f is given in Figure 4b,c. The two binding energies at 710.1 and 724.2 eV in Figure 4b are due to Fe^{3+} of α-Fe_2O_3. Figure 4c displays the Au 4f core level spectrum, showing two doublet peaks at 83.9 eV for Au $4f_{7/2}$ and 87.4 eV for Au $4f_{5/2}$. Compared with the binding energy (84.1 eV) of metallic Au, the Au NPs in this work show a negative shift of ca. 0.2 eV. Zhong et al.[40] have ascribed the negative shift to the strong interaction between the α-Fe_2O_3 support and Au NPs. A similarly phenomenon has also been observed for Au/SnO_2[42] and Pt/Fe_3O_4.[27] Wang and co-workers[27] stated that the negative binding energy shift of Pt was due to electron transfer from Fe_3O_4 to Pt. Importantly, such a strong metal−support interaction has been thought to be a reason for the high activity of CO oxidation catalyst.[28,40,42] It is expected that our Au/α-Fe_2O_3 hybrid nanospindles may be active for CO oxidation, which is later approved by our test.

To test the generality of our one-pot method, we have further adopted the approach to synthesize Pt/α-Fe_2O_3 hybrid nanospindles. The TEM images of the Pt/α-Fe_2O_3 hybrids are shown in Figure 5a,b. Evidently, the Pt NPs are seen supported on the nanospindles, indicating the success of our one-pot procedure in fabricating noble metal/α-Fe_2O_3 hybrid nanomaterials. XPS analysis was also used to characterize the sample. As shown in Figure 5c,d, the significant signals confirm the coexistence of Fe and Pt elements in the hybrids.

Numerous studies have shown that α-Fe_2O_3 is highly active as a gas sensor and CO oxidation catalyst. A multifunctional nanomaterial

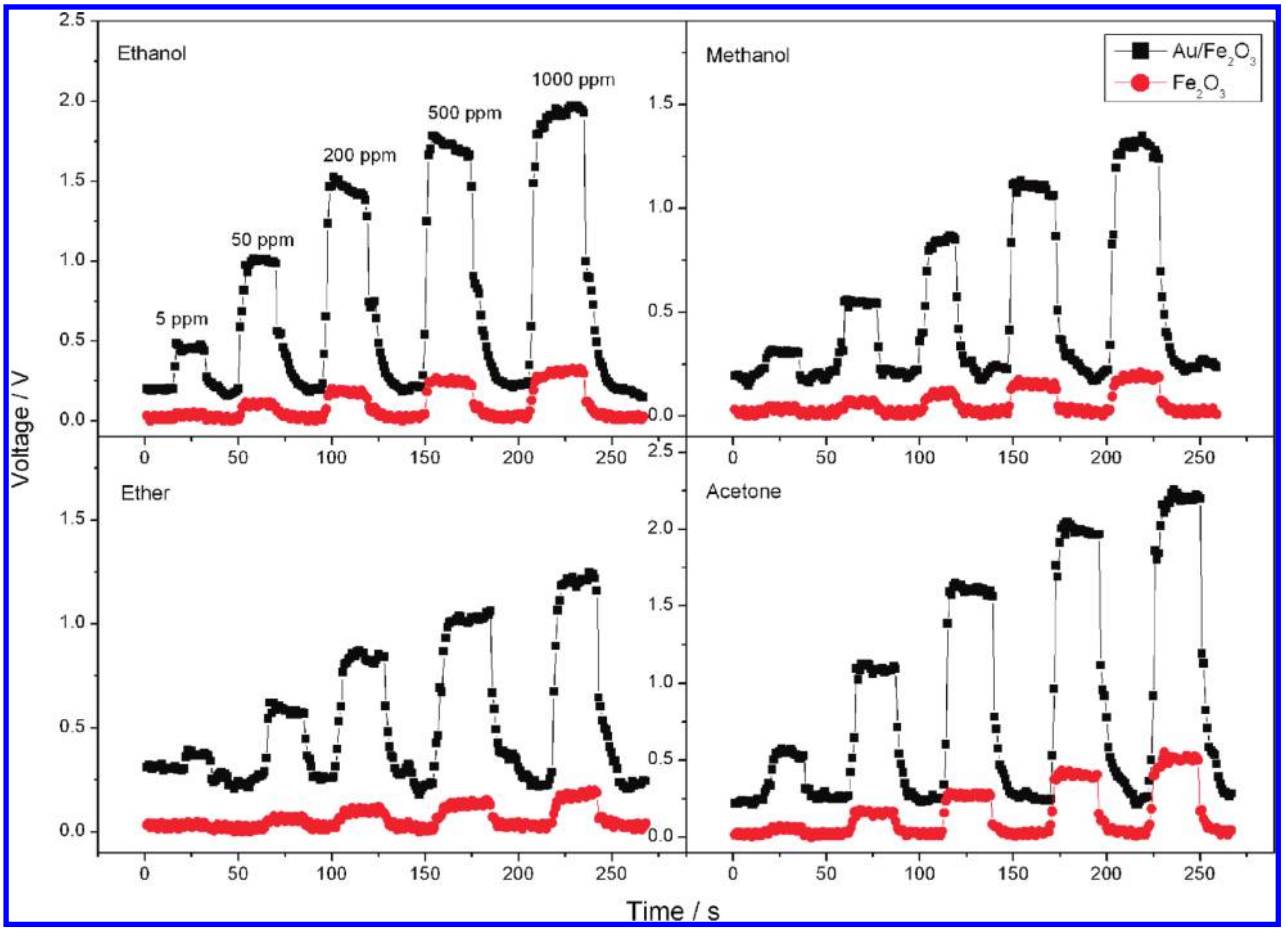

Figure 6. Gas sensing response-recovery curves of pristine α-Fe_2O_3 and hybrid Au/α-Fe_2O_3 nanospindles to four gases (ethanol, methanol, ether, and acetone) at a RH of 20−35%.

is of great significance, as it integrates different functions into one material, which holds great promise for both fundamental and practical perspectives.[5] Inspired by this, we have examined the gas sensing performance and CO oxidation activity of the Au NPs-functionalized α-Fe_2O_3 nanospindles.

Figure 6 compares the gas sensing response-recovery curves of pristine α-Fe_2O_3 and hybrid Au/α-Fe_2O_3 to four different gases (ethanol, methanol, ether, and acetone). It can be seen that the hybrid Au/α-Fe_2O_3 shows significantly enhanced responses compared with pristine α-Fe_2O_3. The response amplitude of Au/α-Fe_2O_3 to all of the test gases exhibits a prominent increase with the increasing gas concentration, while the increase in the response of α-Fe_2O_3 is only slight. Furthermore, as shown in Figure 6, the Au/α-Fe_2O_3 sensor also possesses fast response and recovery speed. The relations between sensor sensitivity and gas concentration are shown in Figure 7. It is observed that the sensor sensitivity of Au/α-Fe_2O_3 is much higher than that of α-Fe_2O_3 toward each gas concentration. Gas sensing tests show that the sensor performances of the α-Fe_2O_3 nanospindles have been dramatically enhanced by the functionalization of Au NPs, which is very promising for gas sensor applications. The improved sensor performance should be related to the active Au NPs, which plays an important role in catalyzing the surface sensing reactions.

Humidity has been reported to affect the properties of gas sensors. For example, Neri and co-workers[42] have investigated the influence of water on the CO response of Au-loaded iron oxide powders. They concluded that water changed the reaction mechanism of CO sensing process. In the presence of water, CO reacts with hydroxyl groups instead of adsorbed oxygen in dry air condition. Thus, we have further tested the ethanol and CO sensing properties of Au NPs-functionalized α-Fe_2O_3 nanospindles at a RH of 63%. Figure S1 of the Supporting Information, SI, shows the dynamic ethanol sensing curves from 5 to 1000 ppm. We can see that the sensor still exhibits fast response and recovery even at a high RH of 63%. Compared with the initial test in Figure 6 (ethanol), the sensor only shows a small decrease in response amplitude toward each concentration. Figure S2 of the SI compares the sensor sensitivities at different RH, revealing that the higher gas concentration the larger decrease in sensor sensitivity.

The CO sensing performance of Au NPs-functionalized α-Fe_2O_3 nanospindles have been examined and the result is shown in Figure S3 of the SI. With the increasing CO concentration from 100 to 1500 ppm, the sensor shows a significant increase in response and also possesses fast response-recovery speed. However, the CO sensing performance is not as good as that for ethanol. Even at a high CO concentration of 1500 ppm, the sensor response is only comparable to that at an ethanol concentration of 50 ppm (Figure S1 of the SI). The sensor sensitivity for CO (inset of Figure S3 of the SI) is 2.16, 3.69, and 5.38 to 100, 300, and 1500 ppm, respectively. This result also indicates that the Au NPs-functionalized α-Fe_2O_3 nanospindles are more sensitive to ethanol than to CO.

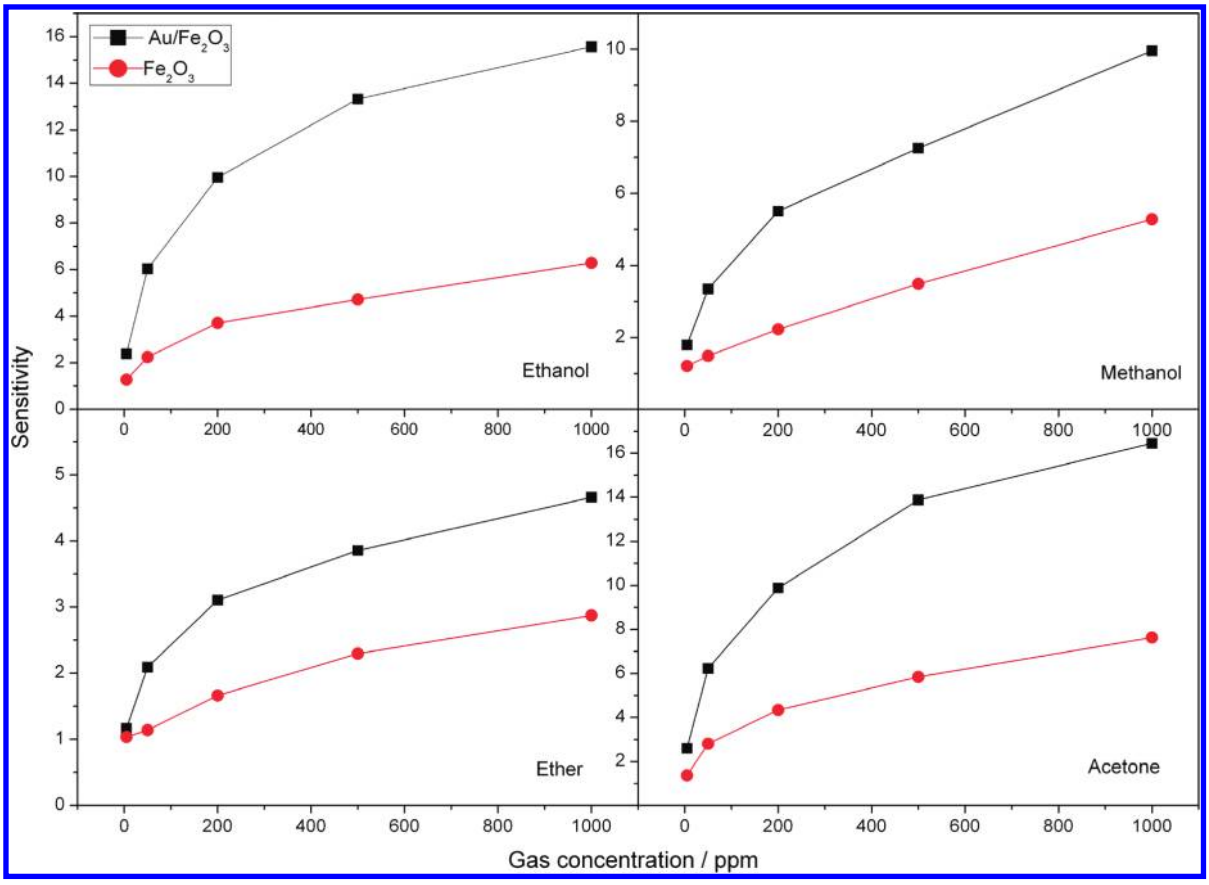

Figure 7. Gas sensor sensitivities of pristine α-Fe_2O_3 and Au/α-Fe_2O_3 hybrid nanospindles to four gases.

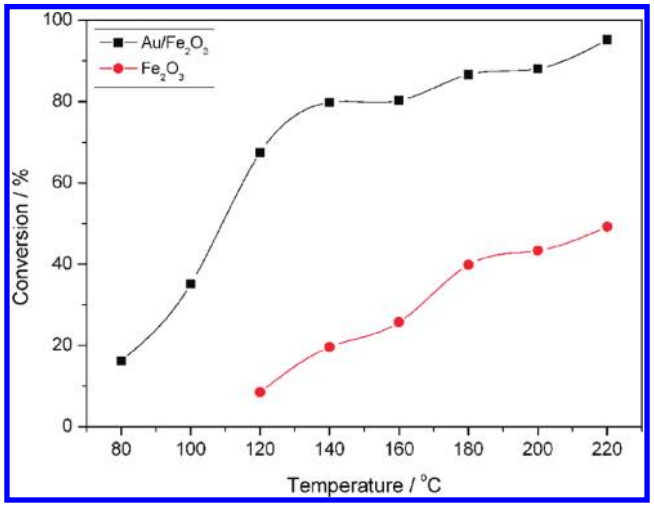

Figure 8. Catalytic performances of pristine α-Fe_2O_3 and Au/α-Fe_2O_3 hybrid nanospindles.

The Au/α-Fe_2O_3 nanospindles were also tested as a catalyst for CO oxidation. The activities of pristine α-Fe_2O_3 and hybrid Au/α-Fe_2O_3 are compared in Figure 8. Obviously, the hybrid Au/α-Fe_2O_3 shows much higher activity. For Au/α-Fe_2O_3, the temperature for half conversion (50%) is about 110 °C, which is far lower than that (ca. 220 °C) of pristine α-Fe_2O_3. The much improved activity of Au/α-Fe_2O_3 should be ascribed to at least two factors. First, as shown in the TEM images of Figure 3, the Au NPs anchored on the nanospindles have an average size of ca. 3 nm. It is widely known that Au NPs with a size smaller than 5 nm are highly active for low temperature CO oxidation,[19,35,40] although Au NPs larger than 15 nm are also active.[43] Second, as revealed by the XPS data, a strong metal−support interaction[40,43] of the hybrid nanospindles may also contribute to the high activity for CO oxidation.

CONCLUSIONS

A facile, green, and general one-pot procedure was established for the synthesis of Au(Pt)-functionalized α-Fe_2O_3 hybrid nanospindles. The synthesis is quite convenient and time-saving, as the conventional functionalization step of the support materials is avoided. Au NPs with a small size were formed in the presence of nontoxic lysine and simultaneously loaded onto α-Fe_2O_3. Importantly, the obtained Au NPs-functionalized α-Fe_2O_3 hybrid nanospindles have a dual function, which shows great promise for both gas sensor and CO oxidation. Our work not only provides a facile and effective route for the preparation of metal-loaded hybrid nanostructures, but also gives an example of using Au NPs/α-Fe_2O_3 hybrid as a multifunctional nanomaterial.

ASSOCIATED CONTENT

Supporting Information. Figure S1, showing the dynamic ethanol sensing curves from 5 to 1000 ppm; Figure S2, comparing the sensor sensitivities at different RH; and Figure S3, showing the CO sensing performance of Au NPs-functionalized

dx.doi.org/10.1021/jp110421v |J. Phys. Chem. C 2011, 115, 5352–5357

α-Fe_2O_3 nanospindles. This material is available free of charge via the Internet at http://pubs.acs.org.

AUTHOR INFORMATION

Corresponding Author
*E-mail: zhangsm@nankai.edu.cn.

ACKNOWLEDGMENT

This work was supported by the National Natural Science Foundation of China (Grant Nos. 20771061 and 20871071) and the Applied Basic Research Programs of Science and Technology Commission Foundation of Tianjin (Grant Nos. 09JCYBJC03600 and 10JCYBJC03900).

REFERENCES

(1) Eder, D. *Chem. Rev.* **2010**, *110*, 1348.
(2) Gomez-Romero, P. *Adv. Mater.* **2001**, *13*, 163.
(3) Shi, W. L.; Zeng, H.; Sahoo, Y.; Ohulchanskyy, T. Y.; Ding, Y.; Wang, Z. L.; Swihart, M.; Prasad, P. N. *Nano Lett.* **2006**, *6*, 875.
(4) Zeng, J.; Huang, J.; Liu, C.; Wu, C. H.; Lin, Y.; Wang, X.; Zhang, S.; Hou, J.; Xia, Y. *Adv. Mater.* **2010**, *22*, 1936.
(5) Zhou, T.; Lu, M.; Zhang, Z.; Gong, H.; Chin, W. S.; Liu, B. *Adv. Mater.* **2009**, *21*, 1.
(6) Guo, S.; Dong, S.; Wang, E. *J. Phys. Chem. C* **2008**, *112*, 2389.
(7) Guo, S.; Dong, S.; Wang, E. *Chem.—Eur. J.* **2009**, *15*, 2416.
(8) Guo, S.; Dong, S.; Wang, E. *J. Phys. Chem. C* **2009**, *113*, 5485.
(9) Guo, S. J.; Li, J.; Ren, W.; Wen, D.; Dong, S. J.; Wang, E. K. *Chem. Mater.* **2009**, *21*, 2247.
(10) Wang, H.; Brandl, D. W.; Le, F.; Nordlander, P.; Halas, N. J. *Nano Lett.* **2006**, *6*, 827.
(11) Jiang, Z. J.; Liu, C. Y. *J. Phys. Chem. B* **2003**, *107*, 12411.
(12) Wang, S.; Jiang, S. P.; White, T. J.; Guo, J.; Wang, X. *Adv. Funct. Mater.* **2009**, *19*, 1.
(13) Wang, S.; Jiang, S. P.; Wang, X. *Nanotechnology* **2009**, *19*, 265601.
(14) Zhai, Y.; Zhai, J.; Wang, Y.; Guo, S.; Ren, W.; Dong, S. *J. Phys. Chem. C* **2009**, *113*, 7009.
(15) Velamakanni, A.; Magnuson, C. W.; Ganesh, K. J.; Zhu, Y.; An, J.; Ferreira, P. J.; Ruoff, R. S. *ACS Nano* **2010**, *4*, 540.
(16) Liu, J.; Fu, S.; Yuan, B.; Li, Y.; Deng, Z. *J. Am. Chem. Soc.* **2010**, *132*, 7279.
(17) Zhang, J.; Liu, X.; Guo, X.; Wu, S.; Wang, S. *Chem.—Eur. J.* **2010**, *16*, 8108.
(18) Liu, X.; Zhang, J.; Guo, X.; Wu, S.; Wang, S. *Nanoscale* **2010**, *2*, 1178.
(19) Zhong, Z. Y.; Lin, J. Y.; Teh, S. P.; Teo, J.; Dautzenberg, F. M. *Adv. Funct. Mater.* **2007**, *17*, 1402.
(20) Zhong, L.-S.; Hu, J.-S.; Cui, Z.-M.; Wan, L.-J.; Song, W.-G. *Chem. Mater.* **2007**, *19*, 4557.
(21) Xu, X.; Cortie, M. B. *J. Phys. Chem. C* **2007**, *111*, 18135.
(22) Xie, Y.; Ding, K. L.; Liu, Z. M.; Tao, R. T.; Sun, Z. Y.; Zhang, H. Y.; An, G. M. *J. Am. Chem. Soc.* **2009**, *131*, 6648.
(23) Zhou, X. Z.; Huang, X.; Qi, X. Y.; Wu, S. X.; Xue, C.; Boey, F. Y. C.; Yan, Q. Y.; Chen, P.; Zhang, H. *J. Phys. Chem. C* **2009**, *113*, 10842.
(24) Zheng, S.-F.; Hu, J.-S.; Zhong, L.-S.; Wan, L.-J.; Song, W.-G. *J. Phys. Chem. C* **2007**, *111*, 11174.
(25) Xu, C.; Wang, B.; Sun, S. *J. Am. Chem. Soc.* **2009**, *131*, 4216.
(26) Yu, H.; Chen, M.; Rice, P. M.; Wang, S. X.; White, R. L.; Sun, S. *Nano Lett.* **2005**, *5*, 379.
(27) Wang, C.; Daimon, H.; Sun, S. *Nano Lett.* **2009**, *9*, 1493.
(28) Wu, B. H.; Zhang, H.; Chen, C.; Lin, S. C.; Zheng, N. F. *Nano Res.* **2009**, *2*, 975.
(29) Ishikawa, T.; Matijevic, E. *Langmuir* **1988**, *4*, 26.
(30) Wang, Y.; Cao, J.; Wang, S.; Guo, X.; Zhang, J.; Xia, H.; Zhang, S.; Wu, S. *J. Phys. Chem. C* **2008**, *112*, 17804.
(31) Wang, G.; Gou, X.; Horvat, J.; Park, J. *J. Phys. Chem. C* **2008**, *112*, 15220.
(32) Chen, J.; Xu, L.; Li, W.; Gou, X. *Adv. Mater.* **2005**, *17*, 582.
(33) Jia, C.-J.; Sun, L.-D.; Yan, Z.-G.; You, L.-P.; Luo, F.; Han, X.-D.; Pang, Y.-C.; Zhang, Z.; Yan, C.-H. *Angew. Chem., Int. Ed.* **2005**, *117*, 4402.
(34) Daniel, M. C.; Astruc, D. *Chem. Rev.* **2004**, *104*, 293.
(35) Hashmi, A. S. K.; Hutchings, G. J. *Angew. Chem., Int. Ed.* **2006**, *45*, 7896.
(36) Min, B. K.; Friend, C. M. *Chem. Rev.* **2007**, *107*, 2709.
(37) Shevchenko, E. V.; Bodnarchuk, M. I.; Kovalenko, M. V.; Talapin, D. V.; Smith, R. K.; Aloni, S.; Heiss, W.; Alivisatos, A. P. *Adv. Mater.* **2008**, *20*, 4323.
(38) Spuch-Calvar, M.; Perez-Juste, J.; Liz-Marzan, L. M. *J. Colloid Interface Sci.* **2007**, *310*, 297.
(39) Liu, X.; Zhang, J.; Guo, X.; Wu, S.; Wang, S. *Nanotechnology* **2010**, *21*, 095501.
(40) Zhong, Z.; Ho, J.; Teo, J.; Shen, S.; Gedanken, A. *Chem. Mater.* **2007**, *19*, 4776.
(41) Ozaki, M.; Kratohvil, S.; Matijevic, E. *J. Colloid Interface Sci.* **1984**, *102*, 146.
(42) Neri, G.; Bonavita, A.; Rizzo, G.; Galvagno, S.; Donato, N.; Caputi, L. S. *Sens. Actuators, B* **2004**, *101*, 90.
(43) Yu, K.; Wu, Z. C.; Zhao, Q. R.; Li, B. X.; Xie, Y. *J. Phys. Chem. C* **2008**, *112*, 2244.